New ternary deep eutectic solvents for effective wheat straw deconstruction into its high-value utilization under near-neutral conditions

Yu-hui Ci, Fei Yu, Cheng-xuan Zhou, Hao-e Mo, Zu-yu Li, Yun-qian Ma* and Li-hua Zang**

School of Environmental Science and Engineering，Qilu University of Technology (Shandong Academy of Sciences)，Jinan 250353，China

*Corresponding authors: Y.Q. Ma; L.H. Zang.

Address: School of Environmental Science and Engineering，Qilu University of Technology (Shandong Academy of Sciences)，Jinan 250353，China

E-mail address: yqma@qlu.edu.cn (Y.Q. Ma); zlh@qlu.edu.cn (L.H. Zang)

Content

1. Material and methods

1.1. Characterization of the DES

The viscosity of DESs was measured on a digital viscometer NDJ-8S (LICHEN, China) using S1 rotor with a speed of 12 and 1.5 rpm. The ^{1}H and ^{13}C NMR spectra of the prepared DES were acquired. The pH value of the DES was measured by diluting 2 ml DES solution obtained either fresh or after four uses with 18 ml deionized water. The pH of the diluted solution was measured using pH meter equipped.

1.2. Extraction method of Alkali lignin

Wheat straw and NaOH solution (8%) were mixed in a high-pressure reaction kettle according to the solid-liquid ratio at 1:10 and heated in a flow oven to 160℃ for 1.5h. After the reaction, the reaction kettle was cooled to room temperature quickly, the solid-liquid separation was carried out with fine gauze, and the filter residue was washed with deionized water until the filtrate became colorless. Use hydrochloric acid to adjust the filtrate pH, when pH > 2, lignin precipitates from the filtrate and precipitates slowly. After standing for 12 hours, the precipitated lignin was separated by centrifugation and washed with deionized water for at least 3 times, and the alkali lignin was obtained after freeze-drying.

1.3. Characterization of the lignin fractions

The weight-average (Mw) and number-average (Mn) molecular weights of the lignin samples were determined by gel permeation chromatography (GPC) (PL-GPC50, Agilent Technologies, USA) with an ultraviolet detector (UV) at 240 nm. NMR spectra of lignin samples were recorded on a Bruker Avance NEO 600 spectrometer at 25℃ in DMSO-d6. FTIR spectra were collected by a IRAffinity-1S (SHIMADZU) spectrometer. Thermogravimetric experiment was performed in TGA5500 Integrated Thermal Gravimetric Analyzer from TA Corporation in America with high purity nitrogen as carrier gas whose flow rate was 25 cm^3/min. About 10 mg material was put in ceramic crucible and heated from room temperature to 700℃ with heating rates of 10℃/min.

1.4. Structure elucidation of the filter residue

The chemical compositions (%, w/w) of the crude fiber residue were determined according to the NREL standard analytical method (NREL/TP-510–42618). The microstructural changes and surface characteristics of the different cellulose-rich substrates were analyzed with a scanning electron microscope (SEM) (Hitachi S4800, Japan) operating at 15 kV acceleration voltages. All samples were coated with gold prior to acquiring images. The diffraction patterns were measured from 5° to 45° by X-ray diffractometer (Ultima IV) at a scanning speed of 2°/min. CrI was calculated using the following formula[1]:

$$\text{CrI} = \frac{I_{002} - I_{am}}{I_{002}} \times 100\%$$

I_{002}, the maximum peak of diffraction near 2θ = 22°

I_{am}, the maximum peak of diffraction near 2θ = 18°

1.5 Enzymatic digestion

Enzymatic hydrolysis was carried out in 30 mL of 0.1 M sodium acetate buffer (pH 4.8) using shaking incubators (SKY-2102C) (Shanghai, China) at 120 rpm and 50℃ for 120 h. Cellulase (15000 FPU/g) was purchased from the Sinopharm Chemical Reagent Co., Ltd and employed at the activity of 30 FPU/g substrate for all the samples. The hydrolysis reaction solution of 200 μL was sampled per 10 h. The intermittent sample was sealed and incubated in a boiling water bath for 5 min to terminate the cellulose hydrolysis reaction, and then centrifuged at 10,000 rpm for 5 min to obtain the supernatant. The supernatant (100 μL) was diluted by ultrapure water, and filtered through a 0.22 μm filter prior to sugar analysis by a HPAEC system with an integral amperometric detector and CarboPac PA20 (3*150 mm, Dionex) analytical column according to the literature. All the hydrolysis experiments were carried out in duplicates. Enzymatic digestibility was calculated using the following formula:

$$Enzymatic\ digestibility = \frac{Quality\ of\ glucose\ after\ Enzymatic\ Hydrolysis \times 0.9}{Quality\ of\ substrate\ before\ Enzymatic\ Hydrolysis} \times 100\%$$

0.9, conversion coefficient of glucose and cellulose

2. DFT calculation parameters

Calculations were performed using Gaussian16 software[2], the functional is M06-2X[3], and the base group is 6-311G(d)[4]. To improve the accuracy of the M06-2X calculations for weak interactions, the DFT-D3 dispersion correction was used[5].

In order to study the weak interaction information in the system, we did AIM (Atoms-in-molecules) analysis on the optimized system[6]. AIM analysis was carried out by Multiwfn software[7]. The strength of hydrogen bond is obtained by AIM analysis of electron density at the bond critical point (BCP) of hydrogen bond according to the empirical formula[8]. The empirical formula is:

$$E\_HB = -223.08 \times \rho(BCP) + 0.7423$$

The hydrogen bonding energy E_HB is in units of kcal/mol and ρ(BCP) is in units of a.u..

2. Tables and Figures

Table S1. Assignments of FTIR bands of lignin.

Frequency/cm^{-1}	Functional group
3403	O-H stretching
2934	C-H stretching
1600	C=O
1506	Aromatic skeletal vibration
1459	C-H deformation
1357	C-O of syringyl ring
1255	C-O of guaiacyl ring
1127	C-O-C glycosidic bond
832	*P*-hydroxyphenyl ring

Table S2. The NMR assignments of major components in the HSQC spectra of DL and AL.

Label	D-Lignin	A-Lignin	assignment
	δ_C/δ_H (ppm)		
B_β	53.7/3.37	ND	C_β−H_β in phenylcoumaran substructures (B)
C_β	53.6/3.06	54.2/3.06	C_β−H_β in β−β′ resinol substructures (C)
-OCH_3	56.2/3.74 and 3.84	56.0/3.74	C−H in methoxyls
A_γ	60.4/3.23-3.65	60.9/3.38	C_γ−H_γ in γ-hydroxylated β-O-4′ substructures (A)
B_γ	63.3/3.69	62.4/3.63	C_γ−H_γ in phenylcoumaran substructures (B)
A‘$_\gamma$	64.7/4.14 and 4.26	ND	C_γ−Hγ in γ-acylated β-O-4′ substructures (A′)
C_γ	70.1/3.94	70.9/3.78-4.22	C_γ−H_γ in β−β′ resinol substructures (C)
A_α(S)	72.3/4.86	ND	C_α−H_α in β-O-4′ substructures (A) linked to a S-unit
A_β(H)	81.3/4.61	ND	C_β−H_β in β-O-4′ substructures (A) linked to a H-unit
A_β(G)	84.3/4.29	ND	C_β−H_β in β-O-4′ substructures (A) linked to a G unit
C_α	84.9/4.73	85.7/4.62	C_α−H_α in β−β′ resinol substructures (C)
A_β(S)	86.6/4.14	ND	C_β−H_β in β-O-4′ substructures linked (A) to a S unit
B_α	87.7/5.48	87.5/5.55	C_α−H_α in phenylcoumaran substructures (B)
$S_{2,6}$	104.4/6.71	104.1/6.67	C_2−H_2 and C_6−H_6 in etherified syringyl units (S)
S‘$_{2.6}$	104.7/7.36	106.6/7.24	C_2−H_2 and C_6−H_6 in etherified syringyl units (S‘)
G_2	111.6/6.95	112.0/7.68	C_2−H_2 in guaiacyl units (G)
PCA_β and FA_β	114.3/6.31	116.7/6.39	C_β−H_β in p-coumarate (PCA) and ferulate (FA)
G_5	115.9/6.84	115.6/6.69	C_5−H_5 in guaiacyl units (G)
G_6	119.6/6.84	119.3/6.77	C_6−H_6 in guaiacyl units (G)
$PCA_{3.5}$	115.4/6.69	115.4/6.68	C_3−H_3 and C_5−H_5 in p-coumarate (PCA)
$H_{2,6}$	128.5/7.12	128.6/7.04	$C_{2,6}$−$H_{2,6}$ in p-hydroxyphenyl units (H)
$PCA_{2,6}$	130.7/7.49	ND	C_2−H_2 and C_6−H_6 in p-coumarate (PCA)
PCA_α and FA_α	145.43/7.57	144.4/7.52	C_α−H_α in p-coumarate (PCA) and ferulate (FA)

Table S3. Molecular weight of two kinds of lignin.

Sample	M_W	M_N	DP (M_W/M_N)
D-Lignin	916	648	1.41358
A-Lignin	1389	814	1.70639

Table S4. Characterization of PBDES before and after recyclability process.

	Original PBDES			Recycled $PBDES_3$	
	$PBDES_1$	$PBDES_2$	$PBDES_3$	1st recycle	2nd recycle
pH	6.96	6.63	6.47	6.51	6.58
Viscosity/mPa·s	75	219	386	795	1439
Recovery rate/%	-	-	-	90.27	91.83

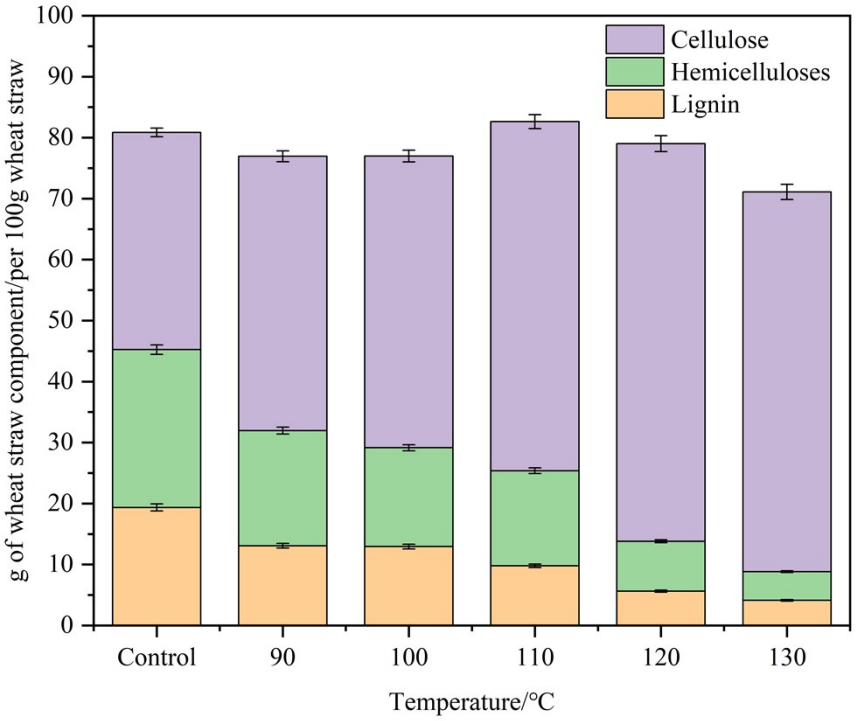

Figure S1. Chemical compositions of original and the pretreated wheat straw at different pretreatment temperatures.

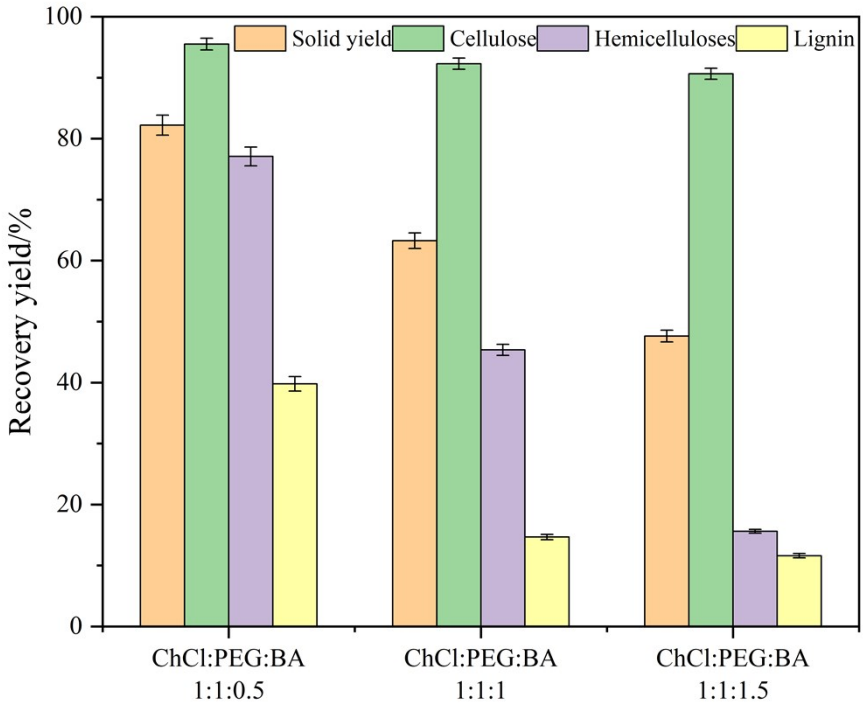

Figure S2. Recovery yield of solid, cellulose, lignin and hemicelluloses at different DES ratios.

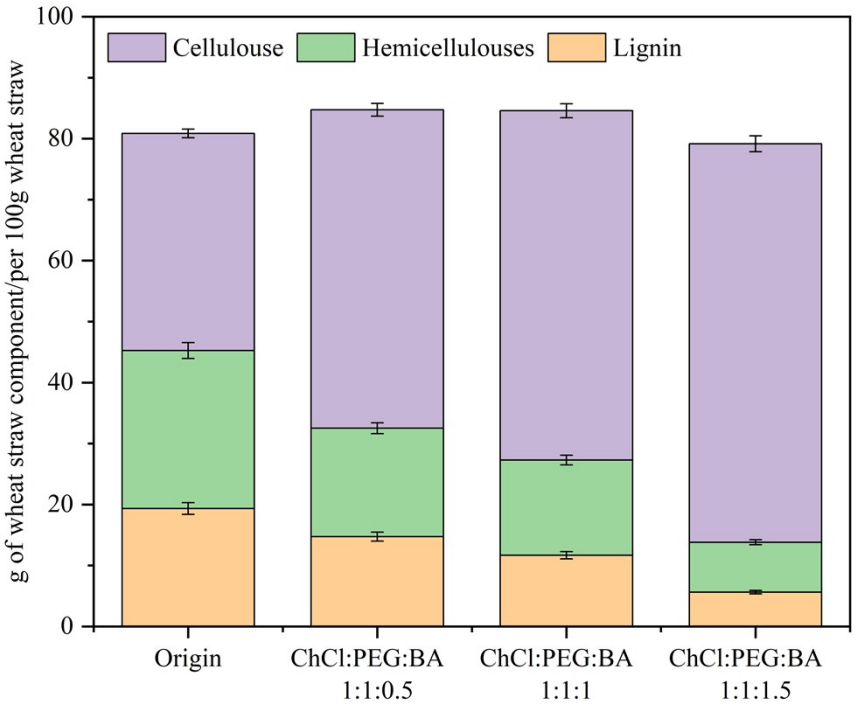

Figure S3. Chemical compositions of original and the pretreated wheat straw at different ratios DES pretreatment.

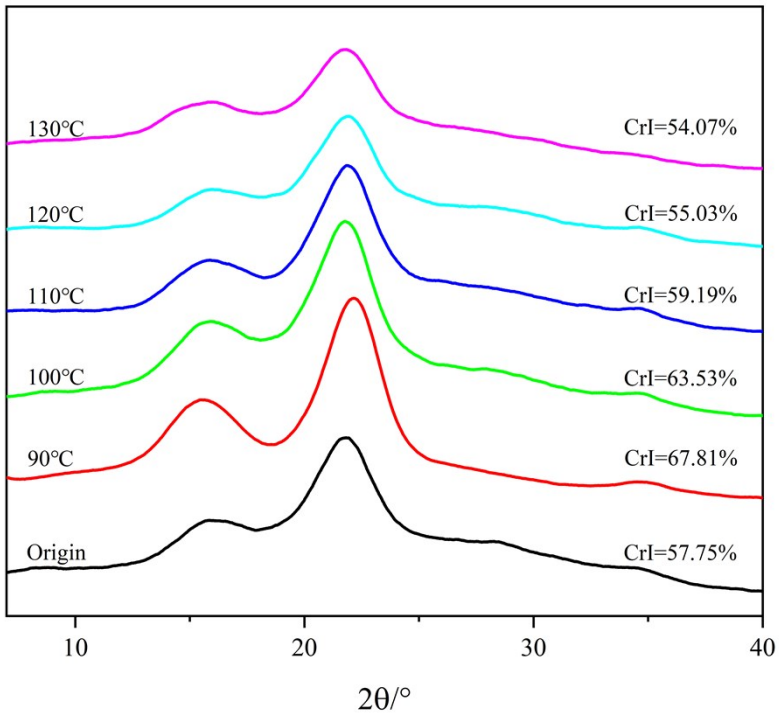

Figure S4. X-ray diffraction of original and the pretreated wheat straw at different pretreatment temperatures.

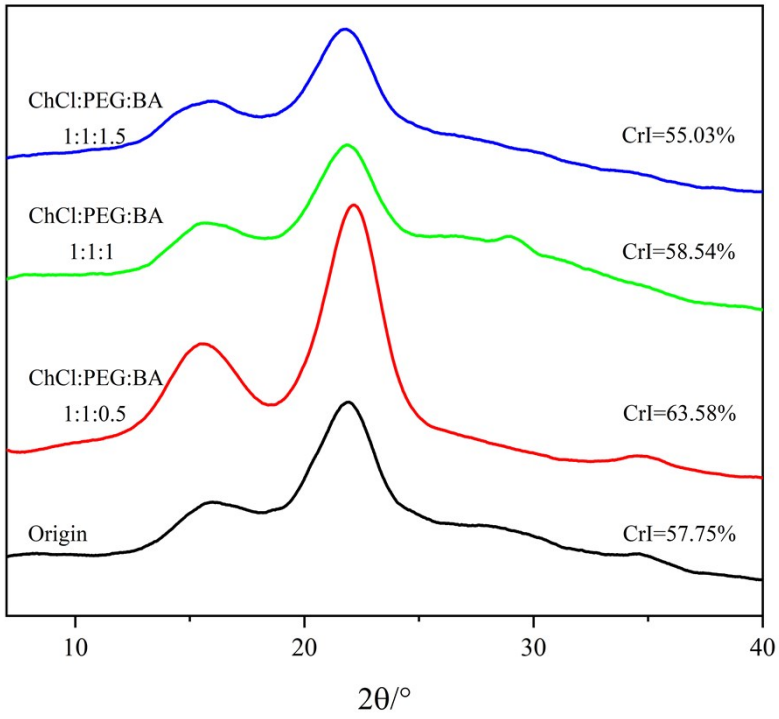

Figure S5. X-ray diffraction of original and the pretreated wheat straw at different ratios of DES pretreatment.

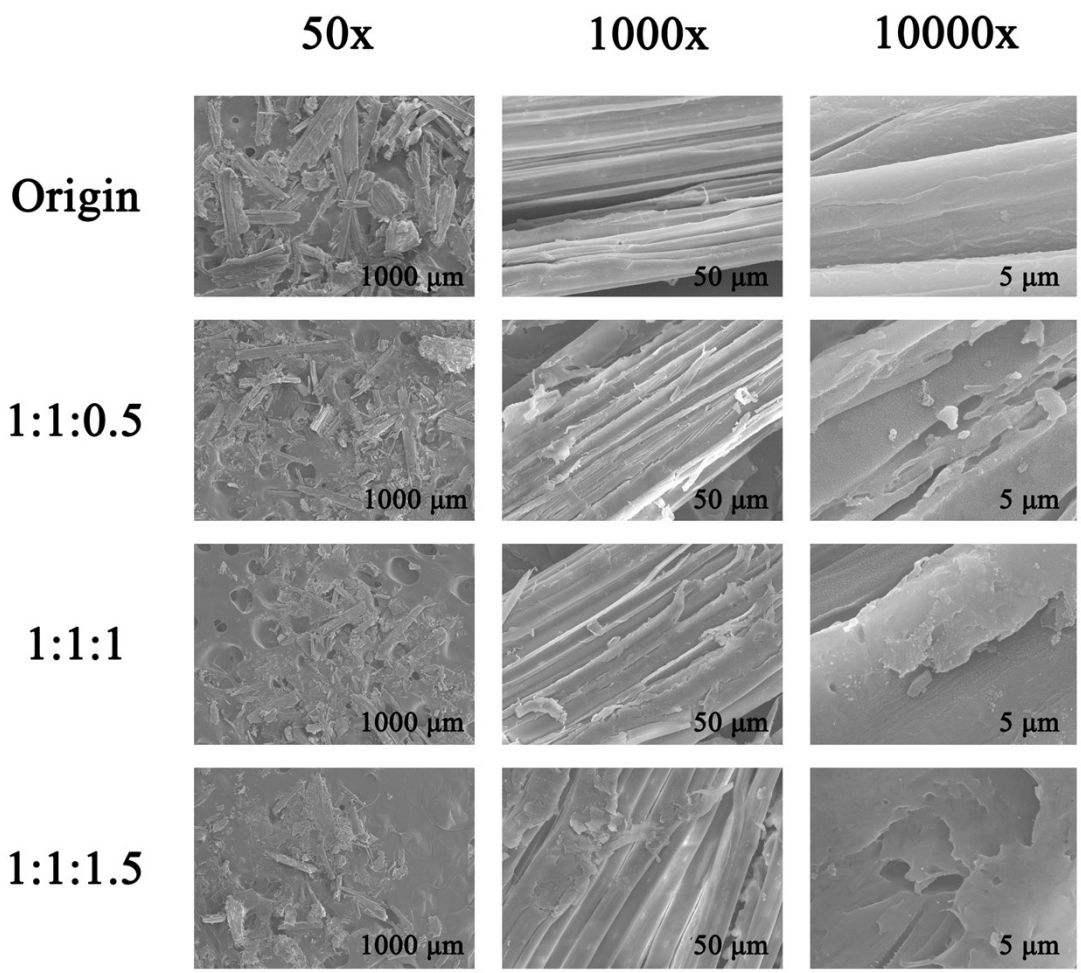

Figure S6. SEM images of the original and the pretreated wheat straw at different ratios of DES pretreatment.

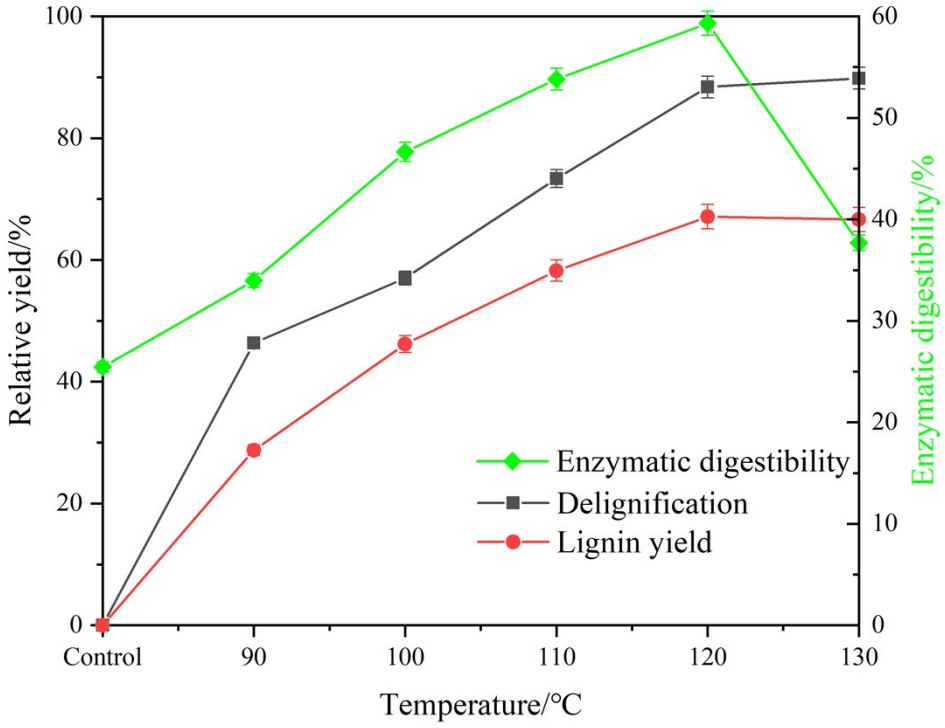

Figure S7. Trends for lignin removal, lignin yield and CrI in relation to enzymatic digestibility under different DES pretreatment temperatures.

Note: Delignification=1-Lignin Recovery

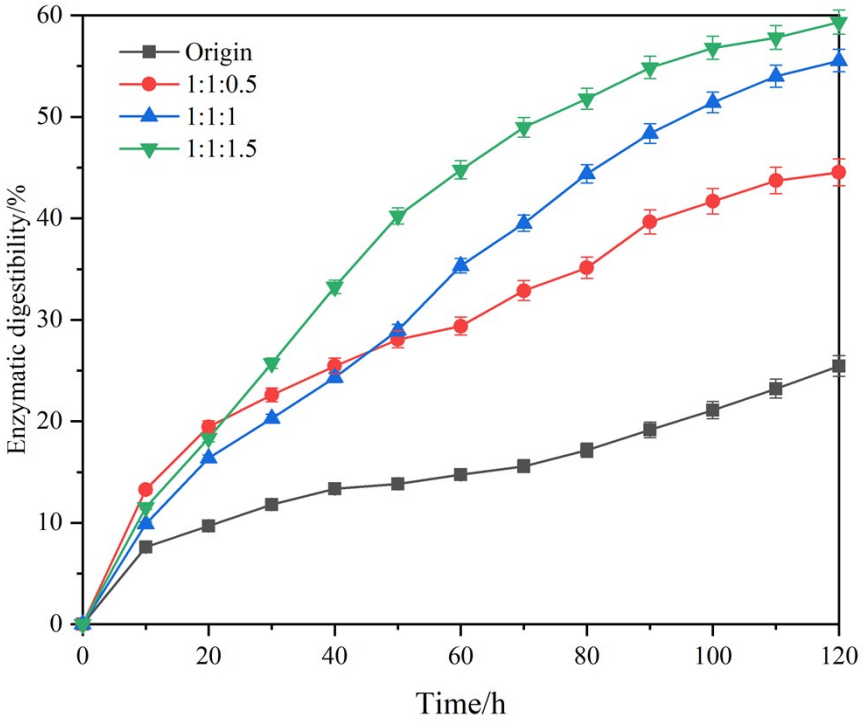

Figure S8. Enzymatic digestibility of original and the pretreated wheat straw at different ratio of DES pretreatment.

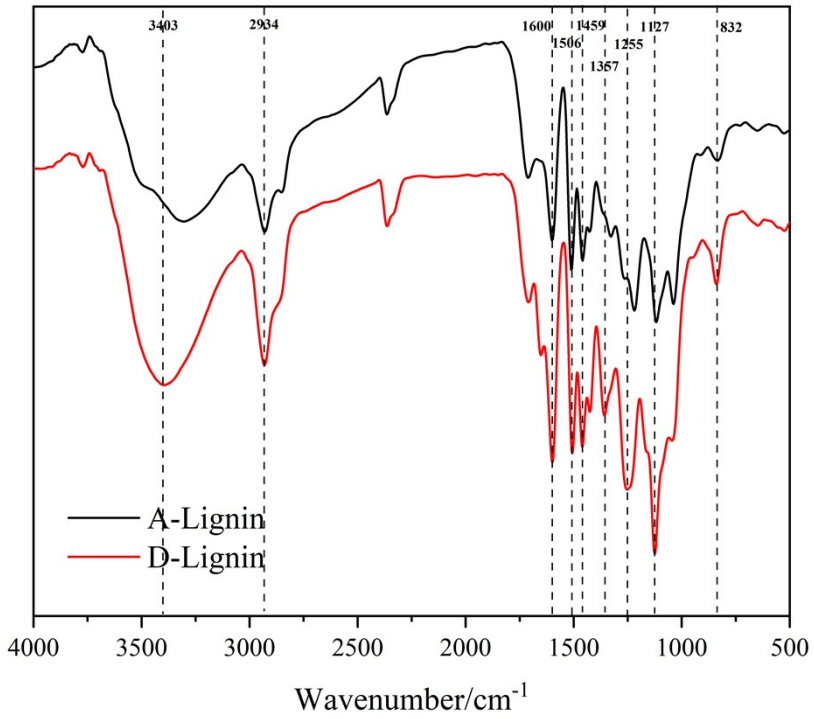

Figure S9. FTIR spectra of DL and AL.

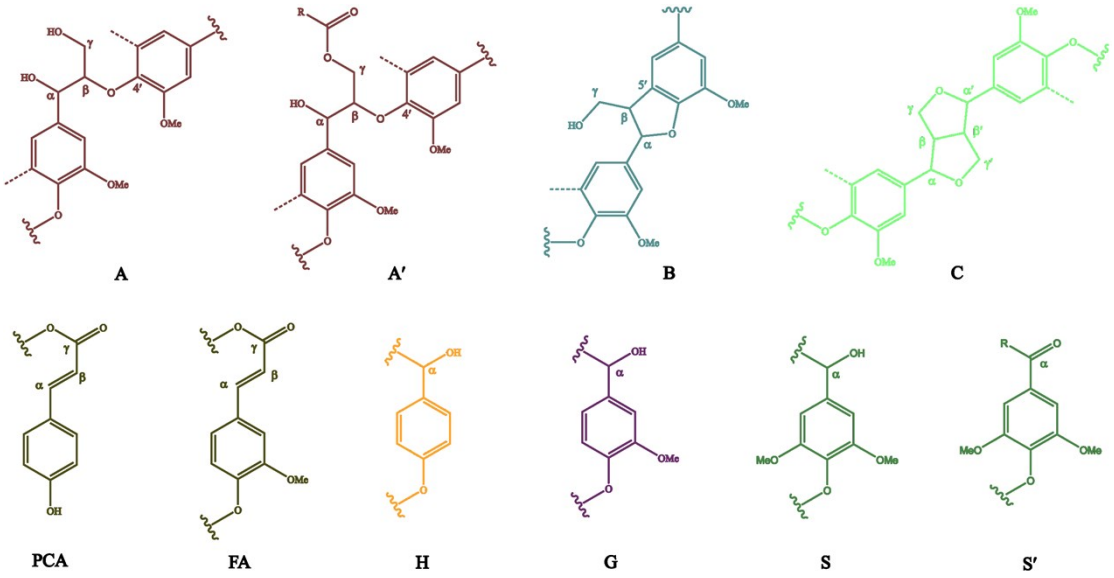

Figure S10. Main structures present in the lignins of wheat straw: (A) β-O-4′ alkyl-aryl ethers; (A′) β-O-4′ alkyl-aryl ethers with acylated γ-OH; (B) phenylcoumarans; (C) resinols; (PCA)p-coumarates; (FA) ferulates; (H)p-hydroxyphenyl units; (G) guaiacyl units; (S) syringyl units.

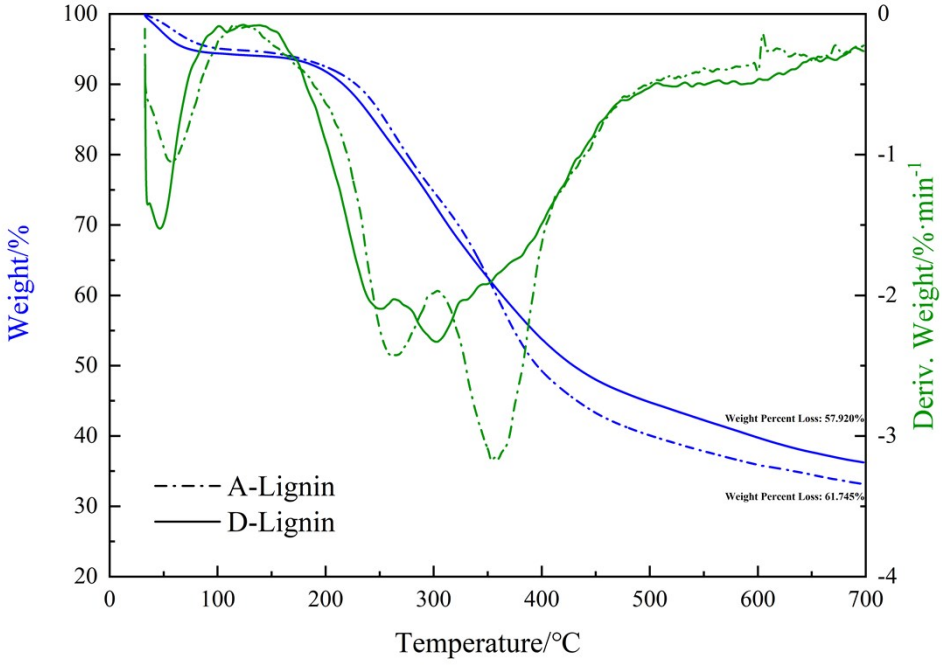

Figure S11. TG and DTG curves of DL and AL.

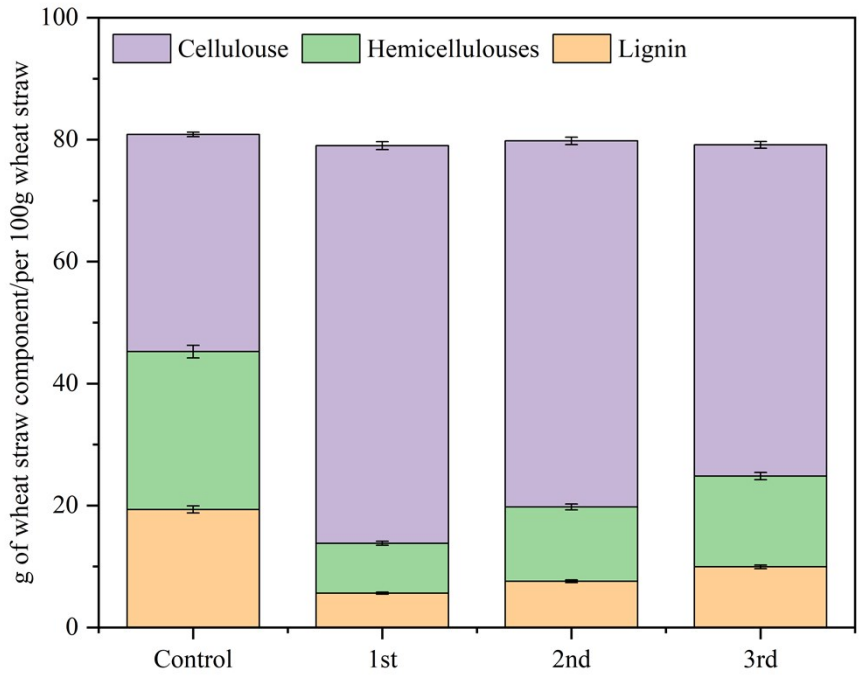

Figure S12. Chemical compositions of the original and pretreated wheat straw at different pretreatment cycle times.

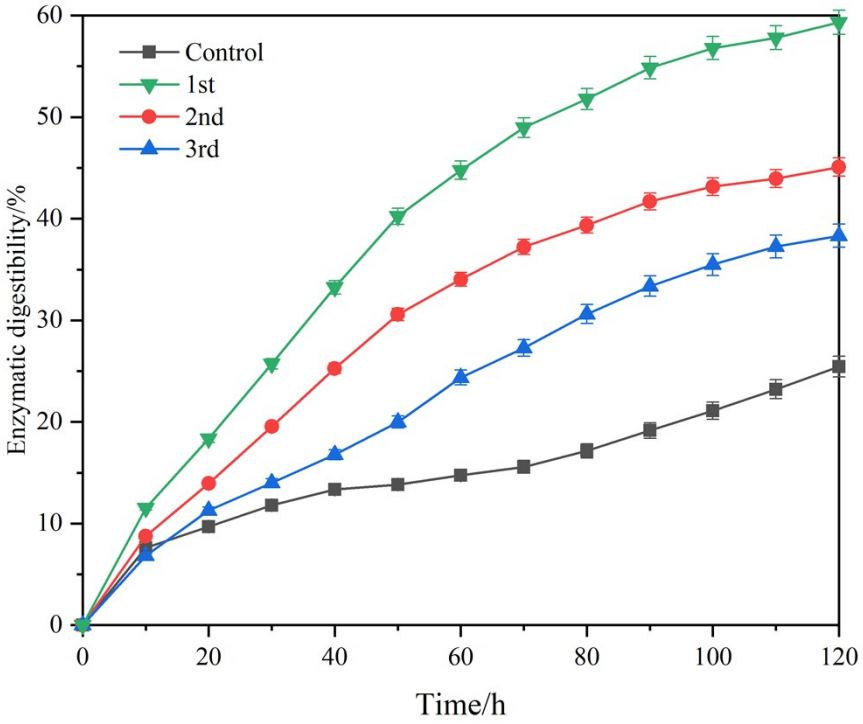

Figure S13. Enzymatic digestibility of the original and the pretreated wheat straw at different pretreatment cycle times.

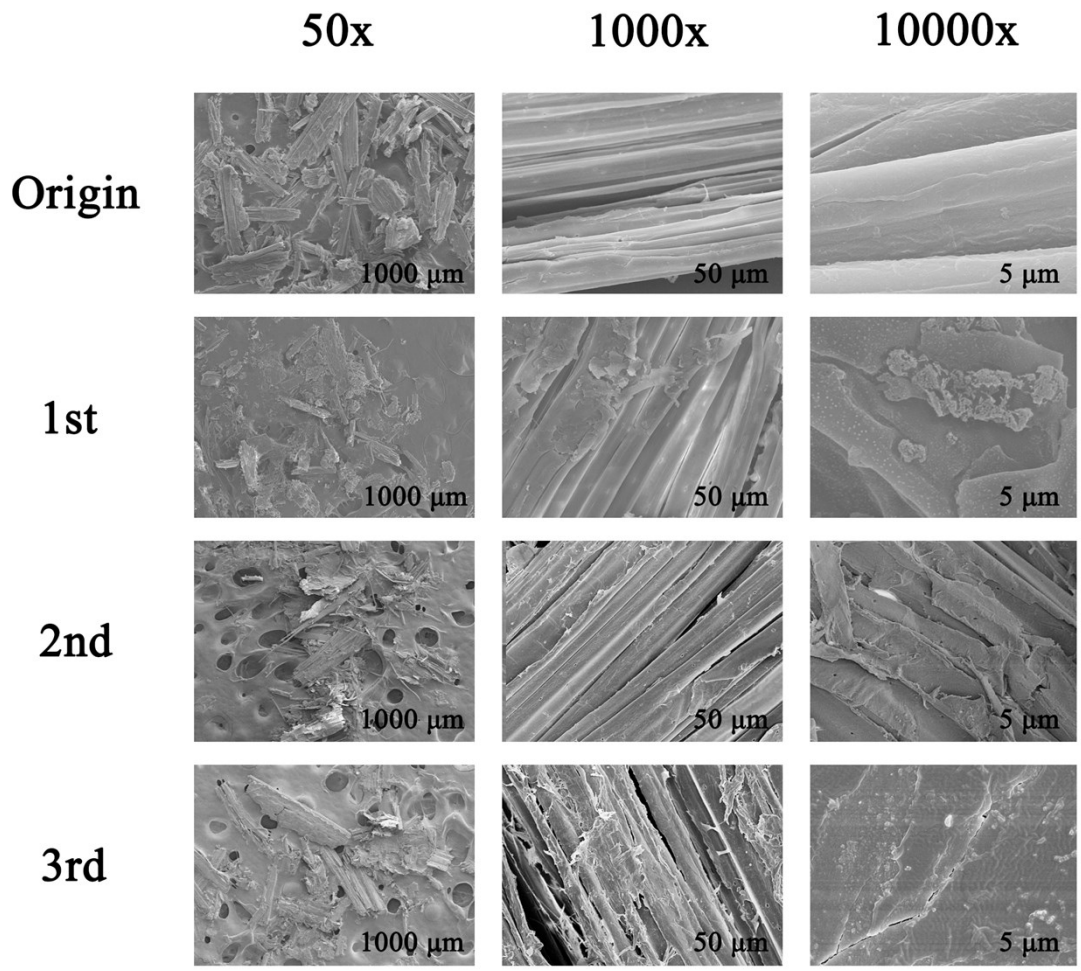

Figure S14. SEM images of original and the pretreated wheat straw sub at different pretreatment cycle times.

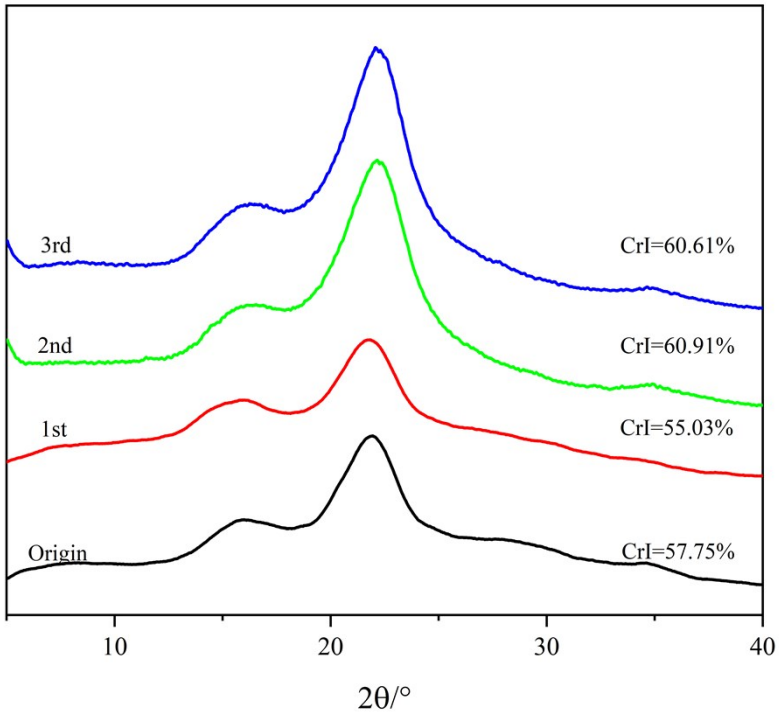

Figure S15. X-ray diffraction of original and the pretreated wheat straw at different pretreatment cycle times.

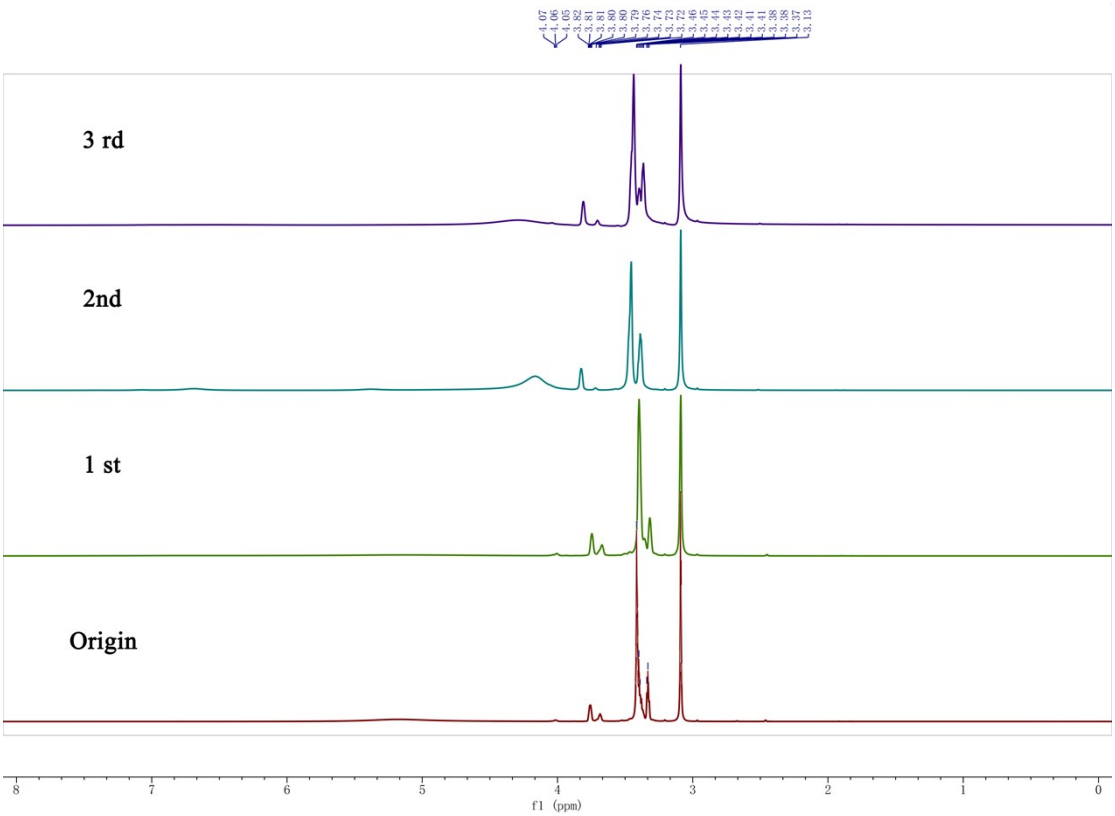

Figure S16. ^{1}H NMR spectra of fresh and the recycled DES at different DES cycles.

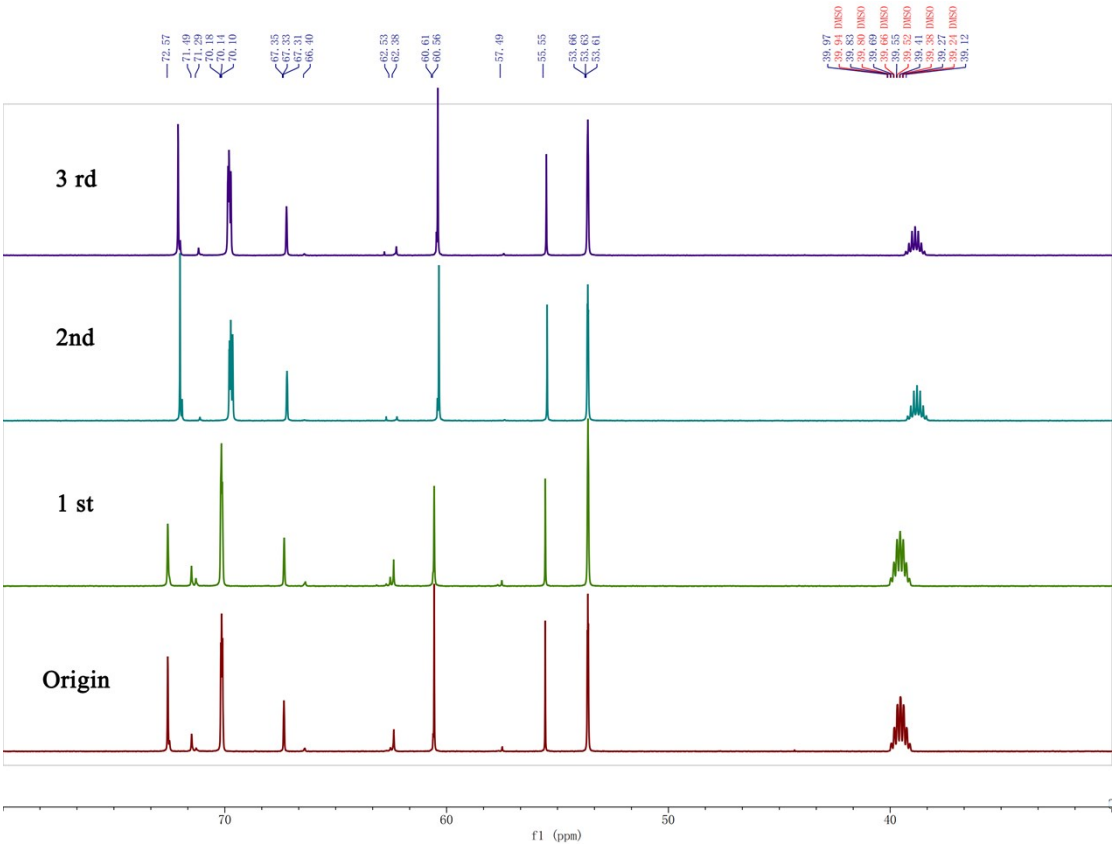

Figure S17. ^{13}C NMR spectra of fresh and the recycled DES at different DES cycles.

References

1. L. Segal, J. J. Creely, A. E. Martin and C. M. Conrad, *Textile Research Journal*, 1959, **29**, 786-794.

2. M. J. Frisch, G. W. Trucks, H. B. Schlegel, G. E. Scuseria, M. A. Robb, J. R. Cheeseman, G. Scalmani, V. Barone, G. A. Petersson, H. Nakatsuji, X. Li, M. Caricato, A. V. Marenich, J. Bloino, B. G. Janesko, R. Gomperts, B. Mennucci, H. P. Hratchian, J. V. Ortiz, A. F. Izmaylov, J. L. Sonnenberg, Williams, F. Ding, F. Lipparini, F. Egidi, J. Goings, B. Peng, A. Petrone, T. Henderson, D. Ranasinghe, V. G. Zakrzewski, J. Gao, N. Rega, G. Zheng, W. Liang, M. Hada, M. Ehara, K. Toyota, R. Fukuda, J. Hasegawa, M. Ishida, T. Nakajima, Y. Honda, O. Kitao, H. Nakai, T. Vreven, K. Throssell, J. A. Montgomery Jr., J. E. Peralta, F. Ogliaro, M. J. Bearpark, J. J. Heyd, E. N. Brothers, K. N. Kudin, V. N. Staroverov, T. A. Keith, R. Kobayashi, J. Normand, K. Raghavachari, A. P. Rendell, J. C. Burant, S. S. Iyengar, J. Tomasi, M. Cossi, J. M. Millam, M. Klene, C. Adamo, R. Cammi, J. W. Ochterski, R. L. Martin, K. Morokuma, O. Farkas, J. B. Foresman and D. J. Fox, *Journal*, 2016.

3. Y. Zhao and D. G. Truhlar, *Theoretical Chemistry Accounts*, 2007, **120**, 215-241.

4. R. Krishnan, J. S. Binkley, R. Seeger and J. A. Pople, *The Journal of Chemical Physics*, 1980, **72**, 650-654.

5. S. Grimme, J. Antony, S. Ehrlich and H. Krieg, *J Chem Phys*, 2010, **132**, 154104.

6. R, F, W and Bader, *Accounts of Chemical Research*, 1985.

7. T. Lu and F. Chen, *Journal of Computational Chemistry*, 2012, **33**, 580-592.

8. S. Emamian, T. Lu, H. Kruse and H. Emamian, *Journal of Computational Chemistry*, 2019, **40**, 2868-2881.